NO Formation during Oxy-Fuel Combustion of Coal and Biomass Chars

3 AUTHORS, INCLUDING:

Anker Degn Jensen
Technical University of Denmark

181 PUBLICATIONS **3,880** CITATIONS

SEE PROFILE

P. Glarborg
Technical University of Denmark

196 PUBLICATIONS **5,691** CITATIONS

SEE PROFILE

NO Formation during Oxy-Fuel Combustion of Coal and Biomass Chars

Ke Zhao,* Anker Degn Jensen, and Peter Glarborg

Department of Chemical and Biochemical Engineering, Technical University of Denmark, Building 229, SøltoftsPlads, 2800 Kgs. Lyngby, Denmark

Ⓢ *Supporting Information*

ABSTRACT: The yields of NO from combustion of bituminous coal, lignite, and biomass chars were investigated in O_2/N_2 and O_2/CO_2 atmospheres. The experiments were performed in a laboratory-scale fixed-bed reactor in the temperature range of 850−1150 °C. To minimize thermal deactivation during char preparation, the chars were generated by in situ pyrolysis at the reaction temperature. The NO yield clearly decreased and the CO yield increased when the atmosphere was altered from O_2/N_2 to O_2/CO_2 at 850 °C, but only small differences in NO and CO yields were observed between the two atmospheres at 1050−1150 °C. To examine how CO influences the NO yield, the effect of CO on NO reduction over char as well as NO reduction by CO over ash was investigated in the fixed-bed reactor. Furthermore, the influence of CO on the homogeneous oxidation of HCN, possibly a product of the char-N oxidation, was evaluated using a detailed chemical kinetic model. The results indicate that CO influences the NO yield from char combustion through two paths at 850 °C: (1) CO accelerates NO reduction over char and (2) CO accelerates HCN oxidation, increasing the possibility of NO reduction over char. Both effects were more pronounced at 850 °C than at 1050−1150 °C. The present work indicates that the effect of CO_2 on NO formation in oxy-fuel combustion in fluidized beds can partly be attributed to heterogeneous reactions, whereas for high-temperature pulverized fuel combustion, CO_2 mainly affects the volatile chemistry.

1. INTRODUCTION

Nitric oxide (NO) is an important pollutant, which participates in the formation of acid rain, photochemical smog, and destruction of ozone in the stratosphere.[1] Combustion processes are the major source of NO, and much research has focused on NO formation and reduction in the past few decades.[1−11] In recent years, the focus on global warming and the Earth's climate has led to several methods to control CO_2 from fossil-fueled power plants. The oxy-fuel combustion technology, using pure O_2 and recycled flue gas instead of air as oxidant, yields a plant with a high CO_2 concentration in the exit stream. Oxy-fuel combustion with separation of CO_2 from the exhaust is considered to be one of the most promising technologies for CO_2 capture and storage.[3,4,7,10] The change from N_2 to CO_2 as the dominant gaseous species may alter the devolatilization, volatile composition, and char characteristics, all of which lead to challenges in NO prediction and control. For this reason, a significant amount of research in NO formation in oxy-fuel combustion has been conducted.[1−3,5]

The NO yield in oxy-fuel combustion is generally lower than in air combustion, both in pulverized fuel[1,8] and circulating fluidized bed facilities,[5,6] but the degree of reduction varies significantly depending on fuel composition, reactor design, experimental parameters, and flue gas recirculation (FGR).[3,4,7,10] There is no doubt that recycling through FGR plays a role in lowering the NO yield in the oxy-fuel combustion.[4,5,8−10] However, in once-through studies, the NO yield often decreased when the gas was altered from O_2/N_2 to O_2/CO_2, indicating a chemical effect of CO_2 on NO formation or reduction. Jiang et al.,[12] Hu et al.,[13] Zhang et al.,[14] Hashemi et al.,[15] and Alvarez et al.[16] all investigated coal combustion in O_2/N_2 and O_2/CO_2 in

entrained flow reactors. Their results showed that the NO yields mostly were considerably lower in O_2/CO_2 than in O_2/N_2, but in some conditions, little difference was seen.

Although the mechanisms of NO formation have been extensively studied,[4,7,17−19] it is difficult to explain these observations because devolatilization, fate of volatile-N, char-N oxidation, and NO reduction over char may all be affected differently in an O_2/CO_2 environment compared to O_2/N_2. Although the effect of oxy-fuel conditions on the volatile yield and composition[20] and on oxidation of HCN, NH_3, and CH_4[21−24] has been investigated in recent years, less is known about char-N oxidation and NO reduction over char in an O_2/CO_2 atmosphere, even though they may play an important role for NO emission.[25,26] Hashemi et al.[15] recently reported a model for the nitrogen chemistry in oxy-fuel combustion of pulverized coal. The model was a chemical reaction engineering type of model with a detailed reaction mechanism for the gas-phase chemistry, together with a simplified description of the mixing of flows, heating and devolatilization of particles, and gas−solid reactions. According to their calculations, differences in the NO yield between oxy-fuel combustion and conventional combustion of pulverized coal can mostly be attributed to the recycling of NO (reburning effect) and to changes in the mixing patterns between fuel and oxygen. For pulverized-fuel combustion at high temperatures, Hashemi et al.[15] claimed that NO is mainly reduced by heterogeneous reactions involving both char and soot, and they called for more work on this chemistry, in particular on

Table 1. Matrix of Research Conditions[a]

set		gas composition (vol)	sample	result
1A	char combustion in N_2	10% O_2 + 90% N_2	bituminous coal/lignite/straw char	Figures 4 and 5
1B	char combustion in CO_2	10% O_2 + 90% CO_2	bituminous coal/lignite/straw char	Figures 4 and 5
1C[b]	aged char combustion in N_2	10% O_2 + 90% N_2	bituminous coal char	Figure 4
2	char combustion in CO_2/N_2	10% O_2 + x% CO_2 + (90 − x)% N_2	bituminous coal char	Figure 6
3	char combustion in CO/N_2	10% O_2 + 3.8% CO + 86.2% N_2	bituminous coal char	Figure 7
4	NO reduction by char	640 ppm of NO + (0−9.4)% CO/CO_2 + N_2	bituminous coal char	Figure 8
5	NO reduction by CO over ash	370 ppm of NO + 6.6% CO + N_2	bituminous coal ash	Figure 9
6	HCN oxidation in $CO/CO_2/N_2$	600 ppm of HCN + 10% O_2 + (0.2−2)% CO/CO_2 + N_2		Figures 10 and 11

[a]The experiments are performed at atmospheric pressure in the 850−1150 °C temperature range. [b]The pyrolysis time in the experiment 1C was 30 min, whereas it was 3 min in other experiments.

the reduction of NO by CO on char at higher temperatures. The recent paper by Wang et al.[27] summarizes much of the earlier work and provides novel results on the effect of char-catalyzed NO reduction by CO at CO concentrations representative for oxy-fuel combustion. However, in line with most previous studies, Wang et al.[27] employed long pyrolysis times for producing their char, resulting in chars with a reactivity that is significantly different compared to chars in real pulverized fuel combustion. It has been found that the reaction rate of NO reduction over chars which experienced short time of thermal deactivation (in second to minute scale)[17,18,28] was generally 10−100 times larger than for chars which were deactivated over longer times (in hour scale).[29−32] For this reason, it is important to conduct experiments at high heating rates and short pyrolysis times to approximate the conditions of real pulverized fuel combustion.

The purpose of this work is to study the NO yield of char-N oxidation in air and oxy-fuel combustion, using chars generated by in situ pyrolysis at the reaction temperature to minimize the thermal deactivation. The experiments were conducted in a laboratory fixed-bed reactor with pulverized char in O_2/N_2 and O_2/CO_2 at 850−1150 °C. The NO yield in different atmospheres is presented in sections 3.2 and 3.3. Furthermore, to investigate how the atmosphere influences the NO yield, the effects of CO on NO reduction over char, NO reduction by CO over ash, and HCN oxidation at different CO concentrations were studied (sections 3.3−3.5).

2. EXPERIMENTAL SECTION

2.1. Fuel and Char Characterization. Table 1 lists the experimental conditions tested. The bituminous coal, lignite, and straw have been characterized in previous work,[33−35] and their proximate and ultimate analyses are shown in Table 2. The straw was grinded and

Table 2. Properties of the Fuels

	straw	bituminous coal	lignite
moisture (wt %)	5.40	3.76	9.92
volatiles (wt % dry)	76.4	25.2	47.7
ash (wt % dry)	4.80	15.3	10.9
C (wt % dry)	43.42	70.3	58.0
H (wt % dry)	5.58	3.85	4.48
N (wt % dry)	0.37	1.76	0.67
S (wt % dry)	0.09	0.66	2.90

sieved to 0.063−0.09 mm. The bituminous coal and lignite were sieved to 0.035−0.045 mm.

To determine the chemical composition of the char used in the experiments, 2 g samples were pyrolyzed in nitrogen in a horizontal laboratory-scale tube reactor placed in an electrically heated three-zone furnace (inner diameter = 8 cm, length = 95 cm), described in detail

elsewhere.[36,37] Once the oven reached the desired temperature, 2 NL/min of nitrogen was used to purge the air for 10 min to create an inert atmosphere. Then the alumina crucible and the sample were pushed into the reactor rapidly. The pyrolysis was continued for 10 min with the nitrogen flow of 2 NL/min. After the pyrolysis, the crucible and the sample were removed to the water-cooled part of reactor. The char was subsequently analyzed, and the composition is given in Table 3. Details of the pyrolysis process are described elsewhere.[33]

2.2. Fixed-Reactor Experiments. The experiments were conducted in a laboratory-scale quartz fixed-bed reactor heated by a three-zone electrical oven, which is shown schematically in Figure 1. The reactor was equipped with a solid feeder device, which allowed sample admission into the reactor under inert conditions without disassembling the reactor. Jensen et al.,[28] Sørensen et al.,[30] and Garijo et al.[17,18] used a similar reactor in previous work. The reaction temperature was measured by a thermocouple 0.5 cm below the porous plate. The temperature profiles are shown in the Supporting Information.

The reactor was heated to the desired temperature, between 850 and 1150 °C. The fuel sample was mixed with 2 g of sand (0.18−0.25 mm) and then introduced into the reactor in an inert nitrogen atmosphere. The purpose of the sand was to assist in the introduction of the fuel sample into the reactor and to provide a constant bed height independent of the char mass to ensure plug flow. To minimize the thermal deactivation of char, the char samples were generated by in situ pyrolysis for 3 min, which is sufficient for the pyrolysis reaction according to CO and CO_2 gas profiles of the outlet gas. The char was then exposed to different gas atmospheres, as described below.

An experiment conducted using a NO/NO_x analyzer (Eco Physics, CLD 700 EL) during char combustion confirmed that no NO_2 was produced. Thus, NO_2 was not measured in the following experiments. Flue gas (1 NL/min) was analyzed for NO, CO, CO_2, SO_2, and O_2. An infrared analyzer (Hartmann & Braun, Uras 3G) was used for CO and CO_2, an ultraviolet analyzer (Hartmann & Braun, Radas 1G) was used for NO and SO_2, and a paramagnetic analyzer was used for O_2. Temporal resolution of all gases was 1 s. The CO and CO_2 yields obtained from concentration−time profile (gas analyzer) were in agreement within 3% with integral GC measurements of the flue gas collected in a gas bag.

NO Reduction over Char in O_2-Free Gas. These experiments were conducted with 10−20 mg of bituminous coal. After the pyrolysis, 1.2 NL/min of 640 ppmv NO/N_2 gas passed through the char sand bed. The NO exit concentration was continuously measured. As a final step in the experiments, oxygen was admitted to burn out the remaining char in the char sand bed, and the char mass was determined from CO and CO_2 profiles.

Char Combustion in O_2/N_2. All char oxidation experiments were conducted with 0.1−20 mg of coal or 1−100 mg of biomass. After the 3 min pyrolysis, a gas mixture of 0.15 NL/min oxygen and 1.35 NL/min nitrogen was admitted to the reactor to combust the char. In addition to assisting in the fuel introduction, the sand served to reduce the increase in char temperature during the char combustion. The increase of gas temperature was less than 15 °C in all experiments. The char consumed was determined by integrating the CO and CO_2 profiles. The NO yield

Table 3. Properties of Chars (wt % Dry)^a

	N	C	H	S	ash	char yield
straw char-850 °C	0.53	73.6	0.91	0.228	17.68	19.74
straw char-1050 °C	0.64	74.9	0.46	0.186	18.52	18.93
straw char-1150 °C	0.72	74.1	0.39	0.277	16.36	14.46
bituminous coal char-850 °C	1.50	74.6	0.78	0.595	18.31	73.57
bituminous coal char-1050 °C	1.23	76.2	0.34	0.759	19.12	73.12
bituminous coal char-1150 °C	1.13	78.5	0.23	0.624	18.84	71.14
lignite char-850 °C	0.69	74.1	0.86	2.9	20.31	47.12
lignite char-1050 °C	0.56	77.0	0.33	3.1	21.11	43.90
lignite char-1150 °C	0.61	77.3	0.20	3.3	21.03	42.78

^{a}Chars were obtained by pyrolyzing the fuels in nitrogen at atmosphere pressure.
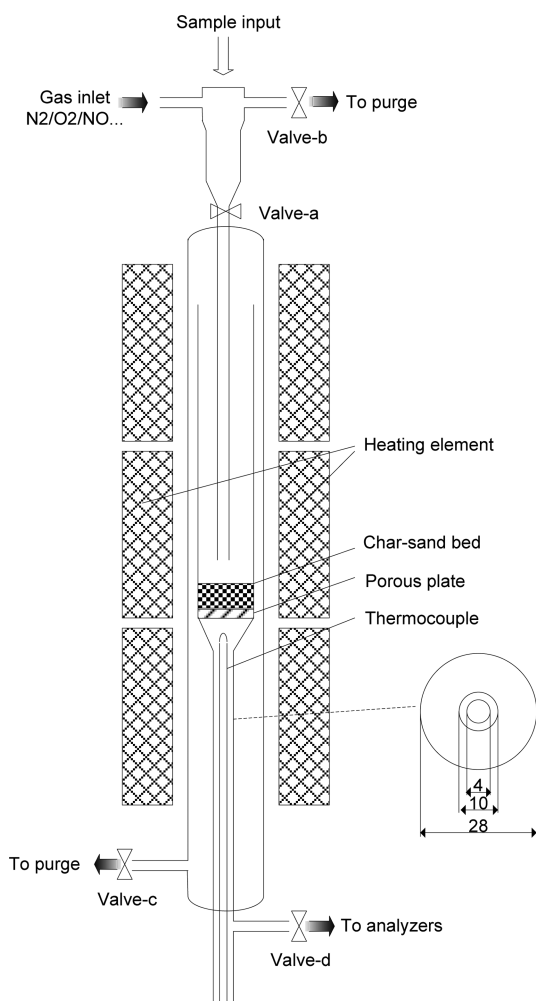
Figure 1. Schematic representation of the fixed-bed reactor. The length scale is millimeter.

from char-N to NO was calculated by the NO concentration profile and the char consumed.

Char Combustion in O₂/CO₂ and O₂/CO/N₂. After the pyrolysis, 1.5 NL/min mixture gases of O_2/CO_2 or $O_2/CO/N_2$ were introduced into the reactor to combust the char. It was not possible to determine the char mass by CO and CO_2 profiles in this case. Instead, the char consumed was determined from the SO_2 profile and the char-S to SO_2 conversion ratio. The char-S to SO_2 conversion ratio in O_2/N_2 was determined from the SO_2, CO, and CO_2 concentration profiles of a large mass sample (6−9 mg of carbon). Each experiment was repeated at least three times, and the uncertainty of the char-S to SO_2 conversion ratio was less than 3.5%. The char-S conversion ratios in O_2/CO_2 were assumed to be the same as that in O_2/N_2. Fleig et al.[38] reported that the

char-S to SO_2 conversion rates in oxy-fuel combustion were lower than in conventional combustion. However, their experiments were conducted in O_2/recycled flue gas. Under these conditions, characterized by longer SO_2 residence times and higher SO_2 concentrations than in air, SO_2 capture by alkali metals in the ash is promoted, leading to a lower char-S to SO_2 conversion rate. In the experiments without recycled flue gas (O_2/CO_2), char-S to SO_2 conversion rates in O_2/N_2 and O_2/CO_2 are similar.[39,40]

3. EXPERIMENTAL RESULTS AND DISCUSSION

3.1. NO Yield. Typical concentration profiles for combustion of bituminous coal char are shown in Figure 2. Higher CO concentrations and lower NO concentrations were achieved in O_2/CO_2 compared to those in O_2/N_2 combustion at 850 °C. Based on the gas profiles and properties of char, the NO yield of char-N, $\overline{\eta_{NO}}$, to NO is calculated from eq 1.

$$\overline{\eta_{NO}} = \frac{\int C_{NO}dt}{m_{char} \times N_{char}} \quad (1)$$

Here, m_{char} is the char mass, C_{NO} is the NO concentration in the flue gas measured by the gas analyzer, and N_{char} is the nitrogen content in char (see Table 3), achieved from experiments in the horizontal tube reactor.

Figure 3 shows the char NO yield as a function of fuel (bituminous coal, lignite, and straw), atmosphere (O_2/N_2 and O_2/CO_2), and pyrolysis time. Figure 3a shows the effect of pyrolysis time on the NO yield. Compared to in situ char (with a pyrolysis time of 3 min), a longer pyrolysis time (30 min) led to considerably higher NO yields at 1050−1150 °C, because the char samples experienced more severe thermal deactivation. For this reason, in situ chars were applied in the present work to minimize thermal deactivation.

Figure 3 shows that the NO yield decreased with increasing char mass in O_2/N_2 atmosphere. The NO yield in the present experiments was a result of NO formation from char-N oxidation and subsequent NO reduction on char while gas flowed through the char sand bed. An increasing char mass led to an increasing reduction when NO passed through the char sand bed. A detailed analysis of the NO yield during char combustion in these conditions is described in our previous research.[28,33] For lignite char combustion in O_2/CO_2 (Figure 3b), the NO yield decreased with an increase of char mass in a way similar to that observed for O_2/N_2 combustion. In evaluating the effect of atmosphere on the NO yield, it is thus important to compare NO yields obtained at similar char mass. For bituminous coal char and straw char (Figure 3a,c), it was difficult to interpret experiments with less than 1 mg of carbon due to weak SO_2 signals in the outlet gas.

The NO yield in O_2/CO_2 combustion was lower compared to that in O_2/N_2 at 850 °C. For example, the NO yield of bituminous coal with 4.5−9.0 mg of carbon decreased from 50 to 65% to 35−40% when the atmosphere was altered from O_2/N_2 to O_2/CO_2. However, there was no obvious difference in NO yields at 1050 and 1150 °C.

Figure 4 shows the CO yields in O_2/N_2 and O_2/CO_2 combustion experiments. The CO yield $\overline{\eta_{CO}}$ is calculated from eq 2.

$$\overline{\eta_{CO}} = \frac{\int C_{CO}dt}{m_{char} \times C_{char}} \quad (2)$$

(a) CO, SO$_2$, and NO

(b) O$_2$ and CO$_2$
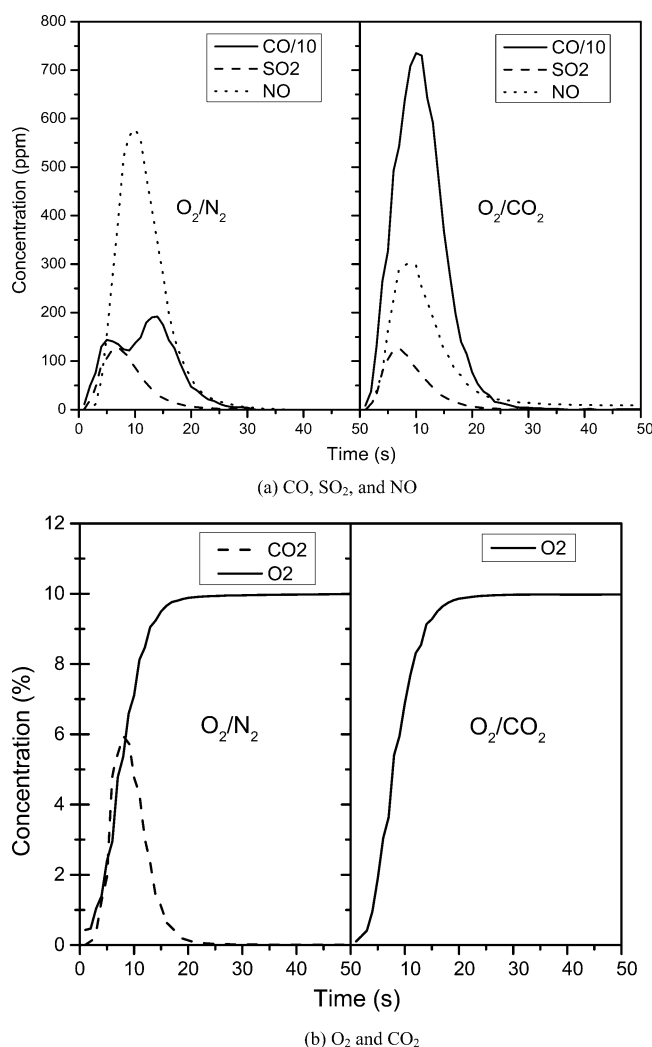
Figure 2. Gas profiles for bituminous coal char in O$_2$/N$_2$ and O$_2$/CO$_2$. Temperature: 850 °C. Char mass: 6.12 mg of carbon in O$_2$/CO$_2$ and 6.27 mg of carbon in O$_2$/N$_2$. Steady-state O$_2$ concentration: 10 vol %. Gas flow: 1.5 NL/min. Temporal resolution: 1 s.

Here, C_{CO} is the CO concentration in the flue gas, C_{char} is the carbon content in the char (Table 3), achieved from experiments in the horizontal tube reactor, and m_{char} is the char mass. For bituminous coal char with 4−9 mg of carbon at 850 °C, the CO yield in O$_2$/CO$_2$ was higher by a factor of 2−5 compared to that of O$_2$/N$_2$. For the straw and lignite at 850 °C, higher CO yields, by a factor of 1.5−3, were achieved in O$_2$/CO$_2$. The presence of CO$_2$ could increase the CO yield at 850 °C by gasification of the char or by inhibition of the CO oxidation, as shown by Gimenez-Lopez et al.[41] At 1050−1150 °C, the CO$_2$ had a much smaller effect on the CO yield than at 850 °C (Figure 4d,e).

Figure 4a also shows that the CO yield decreased significantly with increasing char mass both in O$_2$/N$_2$ and O$_2$/CO$_2$ for bituminous coal at 850 °C. The CO yield at single particle conditions of bituminous coal in O$_2$/N$_2$ (i.e., close to zero mass) was 55%, whereas it was only 8% at 8−8.5 mg of carbon. This may be attributed to the differences in H$_2$O concentration and char particle temperature. The H$_2$O, which originated from hydrogen in the char and could accelerate the CO oxidation, is proportional to the char mass. Thus, a larger mass could produce a higher concentration of H$_2$O, promoting CO oxidation. In addition, a higher char particle temperature is expected in the case of more char mass due to heat release. As a result, CO oxidation to CO$_2$ was enhanced and then led to a lower CO yield.

The experimental results show that a CO$_2$ atmosphere limits the formation of NO from char-N at 850 °C, although the effect is smaller at higher temperatures. The CO yield in O$_2$/CO$_2$ was considerably higher

than in O$_2$/N$_2$ at 850 °C, but the effect of gas atmosphere on CO yield was much smaller at higher temperature. This observation suggests that the effect on NO is associated with the CO level, but other possibilities should be examined. The NO yield in the fixed-bed reactor is controlled by the competition between NO formation and NO reduction. Thermal deactivation,[17,18,28] increasing surface area during char combustion,[42,43] increasing char particle temperature and gas temperature,[18,28] and enhanced reaction rate by the combustion gas[18,30,33,44] are four key phenomena that may influence the NO reduction and then lead to a different NO yield. These are discussed in the following.

Thermal Deactivation. In the present work, the experimental process was designed to ensure that the char experienced the same thermal deactivation regardless of oxidizing atmosphere. As described in section 2.2, the chars were pyrolyzed in the same atmosphere (nitrogen) and for the same time (3 min) in O$_2$/CO$_2$ and O$_2$/N$_2$ experiments.

Char Surface Area. The surface area of the char may increase 1−2 orders of magnitude during combustion, and NO reduction on char has been reported to be proportional to surface area.[42,45] Borrego et al.[46] compared both high and low volatile coal chars in O$_2$/CO$_2$ and O$_2$/N$_2$ combustion. Their results, presented in Figure 5 over the full burnout range from 0 to 100%, show little difference in surface area between chars produced in O$_2$/CO$_2$ and O$_2$/N$_2$ atmospheres, respectively.

Temperature. The char particle temperature and the gas temperature could increase due to heat release during char oxidation. Conceivably the char particle temperature and gas temperature in O$_2$/CO$_2$ are slightly lower than those of O$_2$/N$_2$ due to the increased heat capacity of CO$_2$. However, a minor change in temperature caused by change of atmosphere between O$_2$/CO$_2$ and O$_2$/N$_2$ would have a negligible impact on NO. In a previous study in the same reactor, no significant differences in NO yield were observed over a range of char oxidation rates obtained in 2−10% O$_2$ in O$_2$/N$_2$ at 850−1150 °C.[33]

Gas Environment. Presence of gases such as CO, O$_2$, and SO$_2$ could enhance the NO reduction.[31,47,48] In case of similar char masses in O$_2$/N$_2$ and O$_2$/CO$_2$ such as shown in Figure 2, SO$_2$ and O$_2$ concentrations were similar in the two atmospheres. However, the CO concentration in O$_2$/CO$_2$ was considerably higher than that in O$_2$/N$_2$. Thus, the higher CO concentration probably contributed to the lower NO yield in O$_2$/CO$_2$ combustion. Furthermore, CO$_2$, as the dominant gas in O$_2$/CO$_2$, may possibly play a role for the lower NO yield.

On the basis of these considerations, we believe it is the effect of a changed gas environment (i.e., higher CO and CO$_2$ concentrations) on the chemical reactions, rather than changes in char deactivation, surface area, or temperature, that leads to lower NO yields in O$_2$/CO$_2$ combustion at 850 °C. To examine this further, the effect of CO and CO$_2$ on the NO yield during simultaneous combustion was studied experimentally (section 3.2).

3.2. Effect of CO$_2$ and CO on NO Yield during Char Oxidation. Figure 6 shows the effect of CO$_2$ concentration on the NO yield of bituminous coal char oxidation at 850 °C. To minimize the effect of differences in char mass, a narrow range (5.5−7.5 mg of carbon) was used in all the experiments. The results show that the NO yield decreases with increasing CO$_2$ concentration, from 68% at 0% CO$_2$ (O$_2$/N$_2$ oxidation) to 39% at 90% CO$_2$ (O$_2$/CO$_2$ oxidation). On the other hand, the CO yield increased by a factor of 3, when the CO$_2$ concentration increased from 0 to 90%. These results are consistent with the observations in section 3.1.

To investigate the effect of CO on NO yield during char oxidation, the bituminous coal char was oxidized in O$_2$/N$_2$ and 3.8%CO/O$_2$/N$_2$, respectively. The results are shown in Figure 7. In this experiment, it was important to avoid CO oxidation in gas phase before CO reached the char particle. Empty reactor experiments showed that the CO conversion ratios were 0, 27, and 74% at 750, 800, and 850 °C, respectively. Thus, the reaction temperature was chosen as 750 °C. The results of Figure 7 show that the NO yields were 44−49% in O$_2$/N$_2$ but only 30−33% in a 3.8% CO/O$_2$/N$_2$ atmosphere, confirming that CO could lead to lower NO yield during char oxidation.
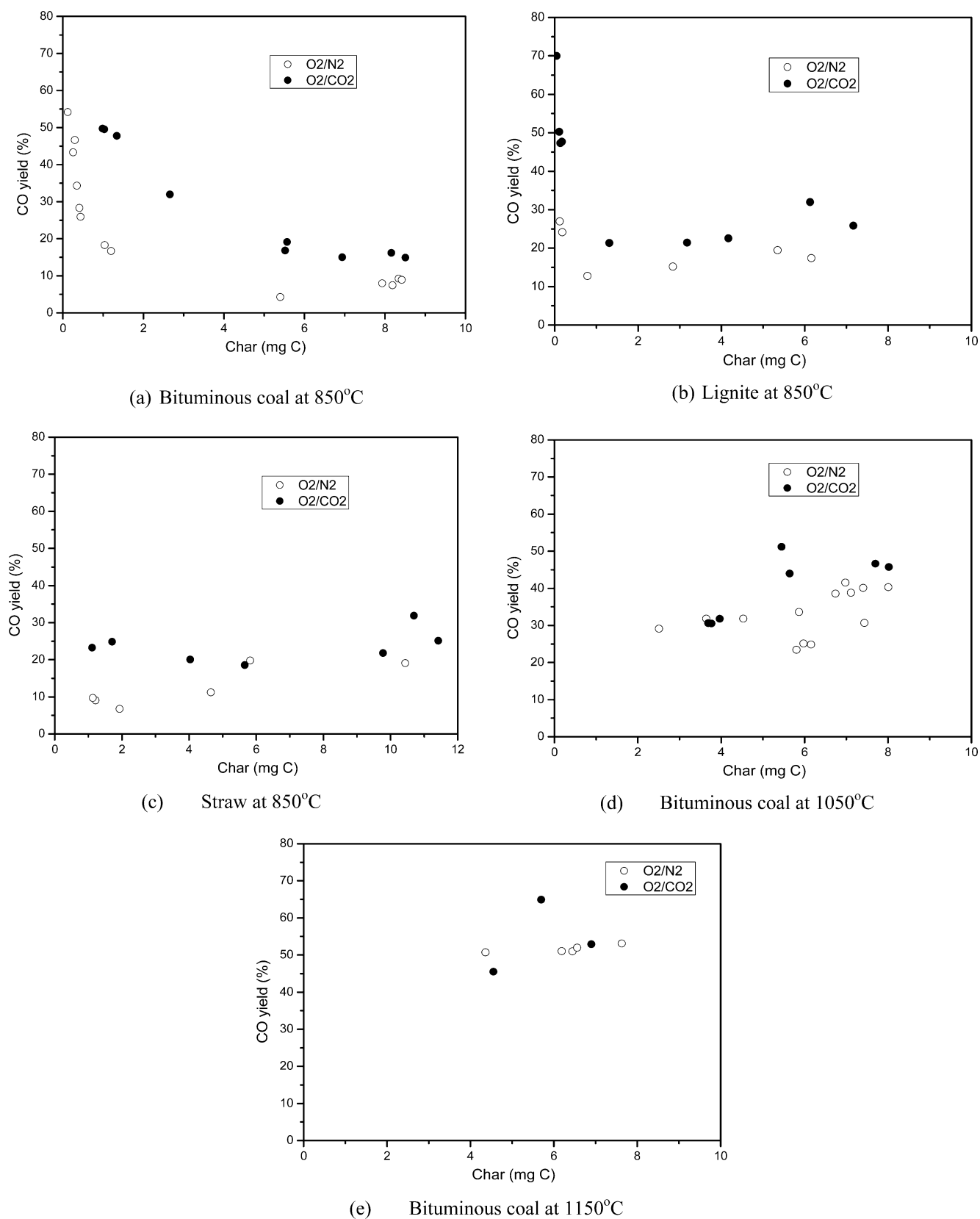
The results in Figures 6 and 7 show that char oxidation in O$_2$/CO$_2$ leads to higher CO concentrations than in O$_2$/N$_2$ at 850 °C. This may explain the lower NO yield achieved when the char is oxidized at
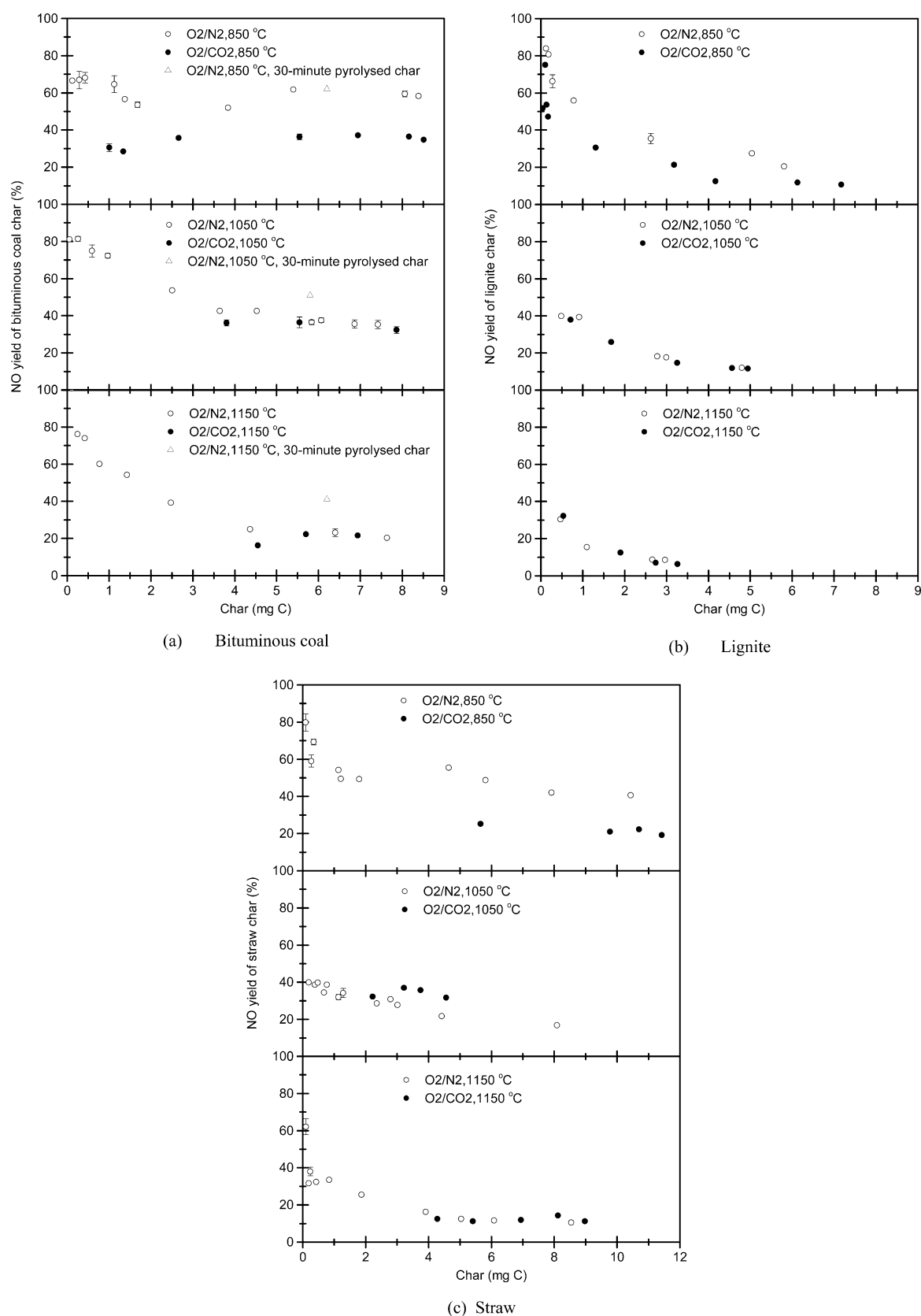
Figure 3. NO yields in O_2/N_2 and O_2/CO_2 combustion experiments. Temperature: 850 °C, 1050 °C, 1150 °C. Steady-state O_2 concentration: 10 vol %. Gas flow: 1.5 NL/min. Selected data for char combustion in O_2/N_2 were drawn from previous work.[33]

higher CO_2 concentrations. The CO concentration in O_2/CO_2 was higher by about a factor of 3 than in O_2/N_2, leading to an enhanced NO reduction.

To examine how the presence of CO influences the NO yield, we investigate the effect of CO on NO reduction over char and ash (sections 3.3 and 3.4). As HCN is believed to evolve as a primary product of char-N
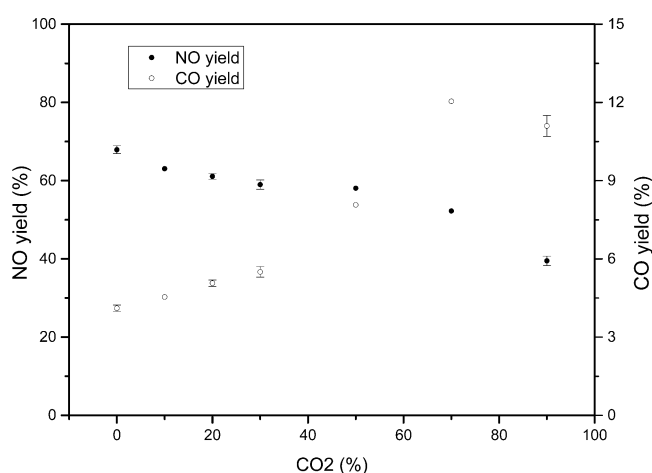
(a) Bituminous coal at 850°C

(b) Lignite at 850°C

(c) Straw at 850°C

(d) Bituminous coal at 1050°C

(e) Bituminous coal at 1150°C

Figure 4. CO yields in O_2/N_2 and O_2/CO_2 combustion (combustion temperature: 850 °C, 1050 °C, 1150 °C. Steady-state O_2 concentration: 10 vol %. Gas flow: 1.5 NL/min.).

oxidation,[22,49,50] the influence of CO and CO_2 on HCN oxidation was simulated using a detailed chemical kinetic model (section 3.5).

3.3. NO Reduction over Char. If the NO reduction over char is assumed to be first order with respect to both NO concentration
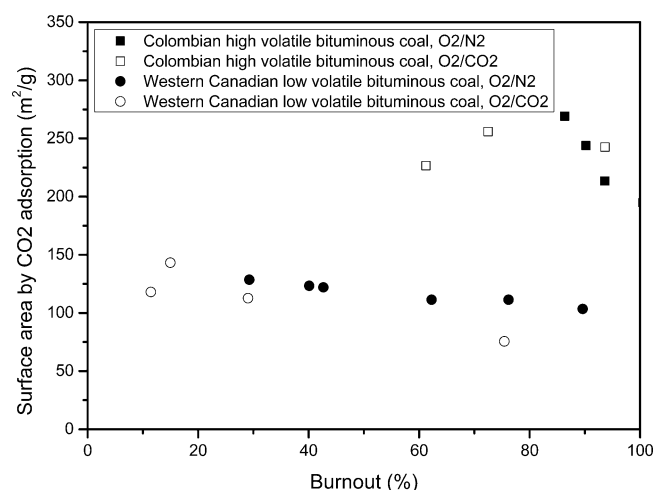
Figure 5. Surface area in O_2/N_2 and O_2/CO_2 at 1300 °C. The data were published by Borrego et al.[46] and are shown here in a modified form.

Figure 6. Effect of CO_2 concentration on NO yield during char oxidation at 850 °C. Fuel: bituminous coal char. Mass: 5.5−7.5 mg of carbon. Inlet gas composition: CO_2 + N_2 + 10 vol % O_2. Combustion temperature: 850 °C. Gas flow: 1.5 NL/min.
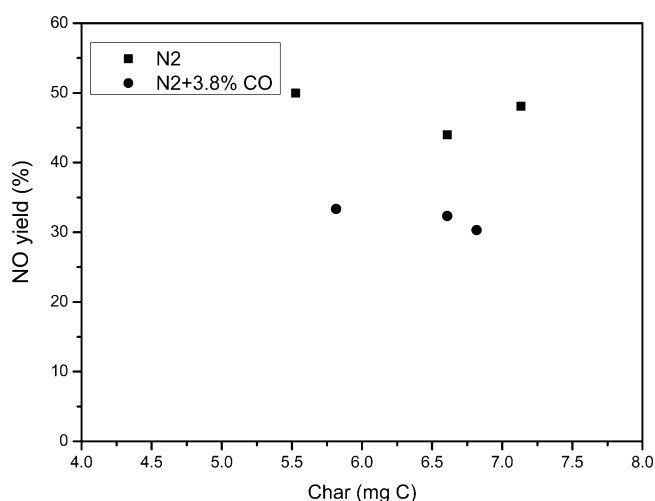

Figure 7. Effect of CO on NO yield during char oxidation. Fuel: bituminous coal char. Combustion temperature: 750 °C. Steady-state O_2 concentration: 10 vol %. Gas flow: 1.5 NL/min.

and carbon mass, the NO reduction rate constant can be obtained from eq 3.

$$(NO)_{red} = k_{NO-char} \times \frac{m_{char}}{V_g} \times X_{NO} \tag{3}$$

Here, $(NO)_{red}$ is the amount of NO reduced by char (in ppm), $k_{NO-char}$ is the NO reduction rate constant (in m³/(kg C)/s) which includes the influence of the CO concentration, m_{char} is the char mass (in kg carbon), V_g is the volumetric gas flow rate (in m³/s), and X_{NO} is the mole fraction of NO (ppm) in the inlet gas.

The effects of CO and CO_2 on NO reduction over char are shown in Figure 8. The results show that CO accelerated the NO reduction over
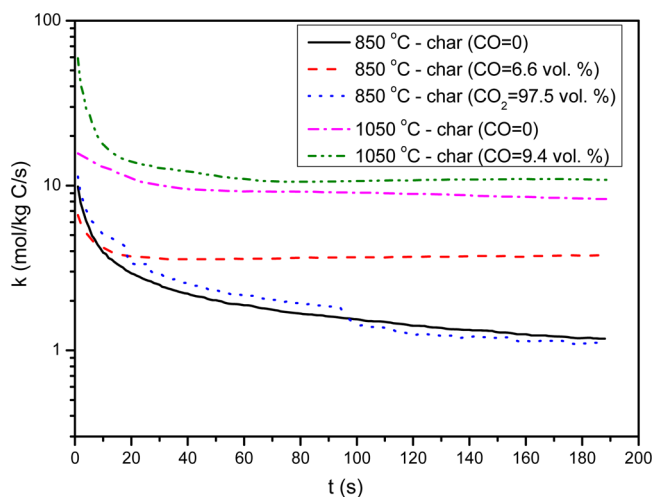
Figure 8. Effect of CO and CO_2 on NO reduction over char. Reaction temperature: 850 °C, 1050 °C. Char mass: 6−10 mg of carbon. Gas flow: 1.2 NL/min. NO concentration: 640 ppmv NO in the inlet gas.

coal char at 850 °C. The reaction rate constant was higher by a factor of 3 for 6.6% CO at 850 °C compared to the 0% CO (pure NO/N_2) atmosphere. However, the effect of CO on NO reduction was almost negligible at 1050 °C. Presence of CO_2, even 97.5%, did not affect the NO reduction rate at 850 °C. At 1050 °C, this experiment was difficult to realize due to significant CO_2 gasification taking place, making it difficult to distinguish the effects of CO and CO_2.

The effect of CO on NO reduction may be due to either a reaction of CO with char (through eqs 4 and 5)[51] or a direct reaction of CO with NO catalyzed by char (through eq 6).[52,53]

$$CO + C(O) \rightarrow CO_2 + C_f \tag{4}$$

$$NO + C_f \rightarrow C(O) + 1/2N_2 \tag{5}$$

$$NO + CO \rightarrow CO_2 + 1/2N_2 \tag{6}$$

$$C(O) \rightarrow CO \tag{7}$$

CO can remove surface carbon oxide $(C(O))$ from the surface at low temperature. As the temperature is increased, the rate of desorption of $C(O)$ to form CO (eq 7) increases rapidly. Thus, the concentration of $C(O)$ will decrease, and the influence of CO on NO reduction through eqs 4 and 5 will decrease significantly. With respect to the catalytic effect of char on NO reduction by CO, char may suffer sintering or catalytic components may be released to the gas-phase during pyrolysis when the temperature reached 1050−1150 °C. Thus, the catalytic effect of char on NO reduction by CO was possibly more pronounced at 850 °C than at 1050−1150 °C.

3.4. NO Reduction by CO over Ash. In these experiments, the pyrolysis and combustion processes were the same as for the char combustion experiments in O_2/N_2 (section 2.2). After combustion, ash remained in the sand bed (defined as fresh ash in Figure 9), and 1.2 NL/min of $NO/CO/N_2$ mixture gas was passed through the char sand bed. The ash
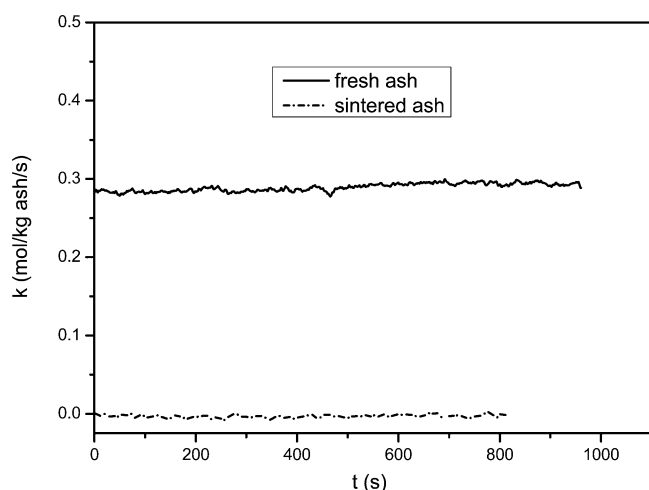
Figure 9. NO reduction by CO over bituminous coal ash. Ash mass: 11.7 mg. Reaction temperature: 850 °C. Gas flow: 1.2 NL/min. Inlet gas composition: 370 ppmv NO + 6.6 vol % CO + N₂. Fresh ash: ash achieved at 850 °C. Sintered ash: the fresh ash heated to 1050 °C and kept for 15 min and then cooled to 850 °C.
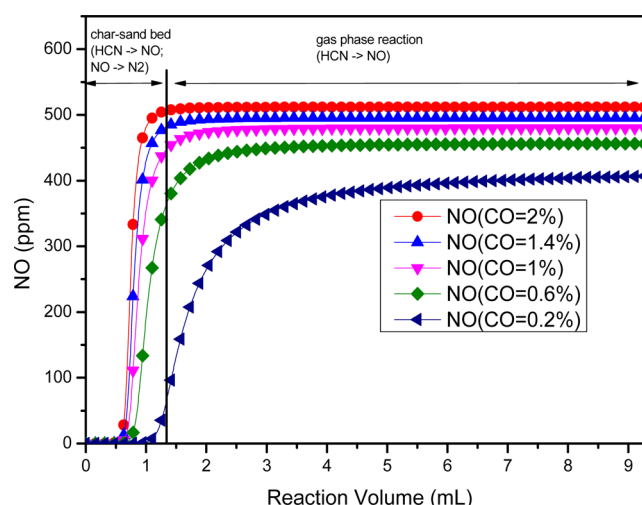

Figure 10. NO profile along the reactor for HCN oxidation. Temperature: 850 °C. Atmosphere: O_2/N_2. Gas flow: 1.5 NL/min. Pressure: 1 atm. Residence time: 91.6 ms. Inlet gas concentration: 600 ppmv HCN + 10 vol % O_2 + 0 ppm of H_2O + 0.2−2.0 vol % CO.

mass was 11.7 mg, calculated from the CO and CO_2 gas profiles and the ash content in char. The sintered ash was achieved by heating the fresh ash to 1050 °C, holding for 15 min, and then cooling to 850 °C.

Assuming the NO reduction over ash to be first order with respect to both NO concentration and ash concentration, the reaction rate could be calculated from eq 8.

$$(NO)_{red,ash} = k_{NO-ash} \times \frac{m_{char}}{V_g} \times X_{NO} \qquad (8)$$

Here, $(NO)_{red,ash}$ is the amount of NO reduced by CO over ash, k_{NO-ash} is the NO reduction rate constant (in $m^3/(kg\ ash)/s$), m_{ash} is the ash mass (in kg ash), V_g is the volumetric gas flow rate (in m^3/s), and X_{NO} is the inlet NO mole fraction (in ppm). The rate constant for NO reduction by CO over ash, derived from the experiments, is shown in Figure 9. The ash showed the catalytic effect on NO reduction by CO at 850 °C. The reaction rate constant of ash was about 0.28 $m^3/(kg\ ash)/s$, which was lower by an order of magnitude compared to char at the same CO concentration. The properties of the ash are shown in Table 4. The catalytic effect can probably be attributed to constituents such as Ca,[27,29,54] Na,[29,55,56] and K.[29,48,57] However, the sintered ash was almost inert for the NO−CO reaction, probably because the catalytic constituents were sintered (Ca) or vaporized to the gas phase (Na and K) while heated to 1050 °C. As a result, NO reduction by CO over ash was much less important at 1050−1150 °C than at 850 °C.

3.5. Effect of CO and CO_2 on HCN Oxidation. Hydrogen cyanide is believed to be an important primary product of char-N oxidation. The higher concentrations of CO and CO_2 in O_2/CO_2 combustion may influence the NO yield via the HCN oxidation process. Thus, the effect of CO and CO_2 on HCN oxidation in the present fixed-bed reactor was evaluated by chemical kinetic modeling using the mechanism developed by Dagaut et al.[22] The calculations were performed using the Plug Flow Reactor Model of Chemkin 4.1.1 software. HCN in the inlet gas was chosen as 600 ppm, comparable to the maximum NO level (Figure 2). The gas flow was 1.5 NL/min and pressure was 1 atm, as in the experiment. The CO gas profiles of char combustion, shown in Figure 2, indicated that the maximum CO concentrations in the outlet gas were 0.19% in O_2/N_2 and 0.74% in O_2/CO_2 combustion, respectively. Thus,
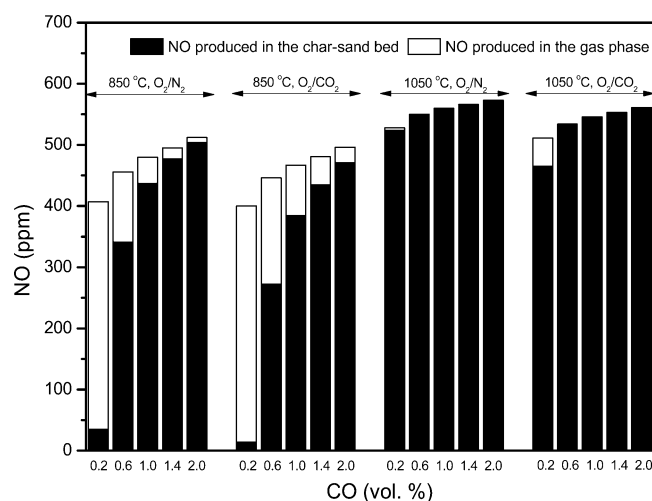
Figure 11. Effect of CO and CO_2 on HCN oxidation. Gas flow: 1.5 NL/min. Pressure: 1 atm. Residence time at 850 °C: 91.6 ms. Inlet gas composition: 600 ppmv HCN + 10 vol % O_2 + 0 ppm of H_2O + 0.2−2.0 vol % CO.

0.2−2% CO was applied in the simulation. The results, shown in Figures 10 and 11, indicate that CO affects both the NO yield and the reaction rate of HCN to NO.

NO Yield. The NO yield from HCN oxidation increased with the increasing CO concentration. As shown in Figure 10, the NO at the outlet increased from 406 ppm (68% NO yield) to 512 ppm (85% NO yield) when CO increased from 0.2% to 2% for HCN oxidation in O_2/N_2 at 850 °C.

HCN Oxidation Rate. The CO accelerates the HCN oxidation rate and leads to an earlier position for NO generation. It is noteworthy that the total reaction volume is 9.42 mL, while the reaction volume of char sand bed is only 1.26 mL. NO produced outside the char sand bed (i.e., the 1.26−9.42 mL part in Figure 10) could not be reduced by char. Thus,

Table 4. Properties of Bituminous Coal Ash

Si	Al	P	Ca	Na	K	Cd	Cr	Cu	Pb	Zn
		(wt % dry)						(wt ppm dry)		
3.4	2.4	0.15	0.86	0.014	0.072	0.03	29.0	11.0	9.6	9.5

the more NO produced in the char sand bed, the more NO can be reduced by char, leading to a lower NO yield.

The overall effect of CO on the NO yield is a result of these two opposite effects. For HCN oxidation at 850 °C in an O_2/N_2 environment, the outlet NO increased from 406 to 512 ppm when CO increased from 0.2% to 2%. However, the NO concentration in the char sand bed increased from 35 ppm at 0.2% CO to 504 ppm at 2% CO. It is likely that the effect of CO on the reaction rate was dominant at 850 °C. As a result, a higher CO concentration would lead to a lower NO yield. At 1050 °C, the HCN oxidation rate was very fast, and almost all NO was produced inside the char sand bed. In this case, the effect of CO on the NO yield and the reaction rate from HCN to NO, respectively, was negligible. Therefore, the CO concentration showed weak effect on NO yield at high temperature. With regard to CO_2, Figure 11 shows that the replacement of N_2 to CO_2 did not change the NO yield significantly.

3.6. Discussion. The motivation for this work was to evaluate the importance of heterogeneous reactions involving char for the differences observed for NO formation in oxy-fuel combustion compared to conventional combustion. On the basis of the results presented in sections 3.3−3.5, we believe that the major impact on the NO yield comes from the enhanced CO levels in oxy-fuel combustion. CO could influence the NO yield in the present reactor through three mechanisms:

Effect of CO on NO Reduction over Char. CO may enhance NO reduction over char through either a reaction of CO with surface species on the char or by a direct reaction of CO with NO catalyzed by the char. The effect of CO on NO reduction over char varied with temperature. CO enhanced the NO reduction rate considerably at 850 °C, although the effect was small at higher temperatures. The results are in good agreement with earlier studies of this reaction conducted with aged chars, where the effect of CO is also reported to decrease with temperature.[27,52,58] An interesting observation by Wang et al.[27] is that the higher the char preparation temperature (and thereby extent of deactivation), the larger is the impact of CO on the reduction of NO.

Effect of CO on NO Reduction over Ash. Ash showed a catalytic effect for NO reduction by CO. However, the rate constant for the ash catalyzed reaction was lower by about an order of magnitude compared to that of char at the same CO concentration at 850 °C. These results are in agreement with data reported by Wang et al.[27] In the present experiments, the char mass was about 4 times higher than the ash mass for the bituminous coal char (Table 2), and NO reduction over char was the dominant NO reduction reaction. However, NO reduction over ash may play a role if the level of catalytic constituents such as Ca, Na, and K is high. Ash from low rank coals has been reported to have a high catalytic activity.[54,56,59,60] The catalyzed reaction may also be important for technologies with high ash proportion, such as circulating fluidized bed combustion, in which the ash is recycled and leads to ash contents of 95−98%.[61,62]

Effect of CO on HCN Oxidation. Presence of CO affects the HCN oxidation in two ways: It may increase the NO yield of HCN oxidation, and it may accelerate the HCN oxidation. The accelerated reaction rate caused a higher probability of NO reduction over char in the present fixed-bed experiments, which may have contributed to a lower NO yield at 850 °C. At higher temperatures, presence of CO had little effect on the HCN oxidation.

We attribute the difference in NO yield between combustion in O_2/N_2 and O_2/CO_2 in the present experiments mainly to the effect of CO on reduction of NO by char. The char combustion experiments (section 3.1) showed that the NO yield decreased, whereas CO was higher by a factor of 2−5 when the gas changed from O_2/N_2 to O_2/CO_2 at 850 °C. At 1050− 1150 °C, there was little difference in CO and NO levels. The present analysis helps to explain the data from Brix et al.,[2] who studied single millimeter-sized combustion of coal char in O_2/N_2 and O_2/CO_2 at 800 °C in a fixed-bed reactor. They found that the NO yield of bituminous coal was considerably lower in O_2/CO_2 compared to O_2/N_2, although for lignite, little difference was observed. Although single particles were used in their experiments, NO reduction over char, enhanced by higher CO levels in O_2/CO_2, still occurred because the char particles were large (2−4 mm) and NO could be reduced in the pore system.

The present results indicate that for oxy-fuel combustion in low-temperature systems like fluidized beds, the higher CO levels would enhance NO reduction on char and thereby lead to lower emissions. However, this mechanism appears to be insignificant at the high temperatures typical of pulverized fuel combustion; under these conditions the char + NO reaction is fast, and the catalyzed step cannot compete.

4. CONCLUSION

An experimental investigation of biomass and coal char combustion has been carried out in O_2/N_2 and O_2/CO_2 at 850−1150 °C in a laboratory-scale fixed-bed reactor. To minimize thermal deactivation during char preparation, the chars were generated by in situ pyrolysis at the reaction temperature. For all fuels, the NO yield decreased significantly and the CO yield increased when the atmosphere was changed from O_2/N_2 to O_2/CO_2 at 850 °C. However, little difference in NO and CO yield was observed in the two atmospheres at 1050−1150 °C. Additional experiments showed that at low temperature (850 °C) CO could lead to lower NO yield during combustion mainly through two paths: enhanced NO reduction over char, as well as effect of CO on HCN oxidation. Both of these effects were more important at 850 °C than at 1050−1150 °C.

■ ASSOCIATED CONTENT

Ⓢ Supporting Information

Temperature profiles along the fixed-bed reactor. This material is available free of charge via the Internet at http://pubs.acs.org.

■ AUTHOR INFORMATION

Corresponding Author

*E-mail: kezh@kt.dtu.dk. Fax: +45 45 88 22 58. Tel.: +45 45252830.

Notes

The authors declare no competing financial interest.

■ REFERENCES

(1) Ndibe, C.; Spoerl, R.; Maier, J.; Scheffknecht, G. *Fuel* **2013**, *107*, 749−756.

(2) Brix, J.; Navascues, L. G.; Nielsen, J. B.; Bonnek, P. L.; Larsen, H. E.; Clausen, S.; Glarborg, P.; Jensen, A. D. *Fuel* **2013**, *106*, 72−78.

(3) Chen, L.; Yong, S. Z.; Ghoniem, A. F. *Prog. Energy Combust. Sci.* **2012**, *38* (2), 156−214.

(4) Toftegaard, M. B.; Brix, J.; Jensen, P. A.; Glarborg, P.; Jensen, A. D. *Prog. Energy Combust. Sci.* **2010**, *36* (5), 581−625.

(5) Jia, L.; Tan, Y.; Anthony, E. J. *Energy Fuels* **2010**, *24*, 910−915.

(6) Czakiert, T.; Sztekler, K.; Karski, S.; Markiewicz, D.; Nowak, W. *Fuel Process. Technol.* **2010**, *91* (11), 1617−1623.

(7) Normann, F.; Andersson, K.; Leckner, B.; Johnsson, F. *Prog. Energy Combust. Sci.* **2009**, *35* (5), 385−397.

(8) Kim, H. K.; Kim, Y.; Lee, S. M.; Ahn, K. Y. *Proc. Combust. Inst.* **2007**, *31*, 3377−3384.

(9) Czakiert, T.; Bis, Z.; Muskala, W.; Nowak, W. *Fuel Process. Technol.* **2006**, *87* (6), 531−538.

(10) Buhre, B. J. P.; Elliott, L. K.; Sheng, C. D.; Gupta, R. P.; Wall, T. F. *Prog. Energy Combust. Sci.* **2005**, *31* (4), 283−307.

(11) Glarborg, P.; Jensen, A. D.; Johnsson, J. E. *Prog. Energy Combust. Sci.* **2003**, *29* (2), 89−113.

(12) Jiang, X. M.; Huang, X. Y.; Liu, J. X.; Han, X. X. *Energy Fuels* **2010**, *24*, 6307−6313.

(13) Hu, Y.; Naito, S.; Kobayashi, N.; Hasatani, M. *Fuel* **2000**, *79* (15), 1925−1932.

(14) Zhang, Y. C.; Zhang, J.; Sheng, C. D.; Liu, Y. X.; Zhao, L.; Ding, Q. Z. *Energy Fuel* **2011**, *25* (3), 1146−1152.

(15) Hashemi, H.; Hansen, S.; Toftegaard, M. B.; Pedersen, K. H.; Jensen, A. D.; Dam-Johansen, K.; Glarborg, P. *Energy Fuels* **2011**, *25* (10), 4280−4289.

(16) Alvarez, L.; Riaza, J.; Gil, M. V.; Pevida, C.; Pis, J. J.; Rubiera, F. *Greenhouse Gases: Sci. Technol.* **2011**, *1* (2), 180−190.

(17) Garijo, E. G.; Jensen, A. D.; Glarborg, P. *Combust. Flame* **2004**, *136* (1−2), 249−253.

(18) Garijo, E. G.; Jensen, A. D.; Glarborg, P. *Energy Fuels* **2003**, *17* (6), 1429−1436.

(19) Jensen, P. A.; Frandsen, F. J.; Dam-Johansen, K.; Sander, B. *Energy Fuels* **2000**, *14* (6), 1280−1285.

(20) Rathnam, R. K.; Elliott, L. K.; Wall, T. F.; Liu, Y.; Moghtaderi, B. *Fuel Process. Technol.* **2009**, *90* (6), 797−802.

(21) Skreiberg, O.; Kilpinen, P.; Glarborg, P. *Combust. Flame* **2004**, *136* (4), 501−518.

(22) Dagaut, P.; Glarborg, P.; Alzueta, M. U. *Prog. Energy Combust. Sci.* **2008**, *34* (1), 1−46.

(23) Glarborg, P.; Bentzen, L. L. B. *Energy Fuels* **2008**, *22* (1), 291−296.

(24) Mendiara, T.; Glarborg, P. *Combust. Flame* **2009**, *156* (10), 1937−1949.

(25) De Soete, G. G. *Symp. (Int.) Combust., [Proc.]* **1991**, *23* (1), 1257−1264.

(26) Harding, A. W.; Brown, S. D.; Thomas, K. M. *Combust. Flame* **1996**, *107* (4), 336−350.

(27) Wang, C. A.; Du, Y. B.; Che, D. F. *Energy Fuels* **2012**, *26* (12), 7367−7377.

(28) Jensen, L. S.; Jannerup, H. E.; Glarborg, P.; Jensen, A.; Dam-Johansen, K. *Proc. Combust. Inst.* **2000**, *28*, 2271−2278.

(29) Aarna, I.; Suuberg, E. M. *Fuel* **1997**, *76* (6), 475−491.

(30) Sørensen, C. O.; Johnsson, J. E.; Jensen, A. *Energy Fuels* **2001**, *15* (6), 1359−1368.

(31) Dong, L.; Gao, S.; Xu, G. *Energy Fuels* **2010**, *24*, 446−450.

(32) Wang, X.; Si, J.; Tan, H.; Zhao, Q.; Xu, T. *Bioresour. Technol.* **2011**, *102* (16), 7401−7406.

(33) Zhao, K.; Glarborg, P.; Jensen, A. D. *Energy Fuels* **2013**, *27* (12), 7817−7826.

(34) Qin, K.; Lin, W.; Faester, S.; Jensen, P. A.; Wu, H.; Jensen, A. D. *Energy Fuels* **2013**, *27* (1), 262−270.

(35) Qin, K.; Lin, W.; Jensen, P. A.; Jensen, A. D. *Fuel* **2012**, *93* (1), 589−600.

(36) Lang, T.; Jensen, A. D.; Jensen, P. A. *Energy Fuels* **2005**, *19* (4), 1631−1643.

(37) Zheng, Y.; Jensen, A. D.; Glarborg, P.; Sendt, K.; Haynes, B. S. *Proc. Combust. Inst.* **2009**, *32*, 1973−1980.

(38) Fleig, D.; Normann, F.; Andersson, K.; Johnsson, F.; Leckner, B. *Energy Procedia* **2009**, *1* (1), 383−390.

(39) Li, W.; Li, S.; Ren, Q.; Tan, L.; Li, H.; Liu, J.; Lu, Q. *Energy Fuels* **2014**, *28* (2), 1249−1254.

(40) Kazanc, F.; Khatami, R.; Crnkovic, P. M.; Levendis, Y. A. *Energy Fuels* **2011**, *25* (7), 2850−2861.

(41) Gimenez-Lopez, J.; Martinez, M.; Millera, A.; Bilbao, R.; Alzueta, M. U. *Combust. Flame* **2011**, *158* (1), 48−56.

(42) Calo, J. M.; Suuberg, E. M.; Aarna, I.; Linares-Solano, A.; de Lecea, C. S. M.; Illan-Gomez, M. J. *Energy Fuels* **1999**, *13* (3), 761−762.

(43) Alvarez, D.; Borrego, A. G. *Energy Fuels* **2007**, *21* (2), 1085−1091.

(44) Dong, L.; Gao, S.; Song, W.; Xu, G. *Fuel Process. Technol.* **2007**, *88* (7), 707−715.

(45) Illangomez, M. J.; Linaressolano, A.; Delecea, C. S.; Calo, J. M. *Energy Fuels* **1993**, *7* (1), 146−154.

(46) Borrego, A. G.; Alvarez, D. *Energy Fuels* **2007**, *21* (6), 3171−3179.

(47) Suzuki, T.; Kyotani, T.; Tomita, A. *Ind. Eng. Chem. Res.* **1994**, *33* (11), 2840−2845.

(48) Illan-Gomez, M. J.; de Lecea, C. S. M.; Linares-Solano, A.; Radovic, L. R. *Energy Fuels* **1998**, *12* (6), 1256−1264.

(49) Wargadalam, V. J.; Loffler, G.; Winter, F.; Hofbauer, H. *Combust. Flame* **2000**, *120* (4), 465−478.

(50) Gimenez-Lopez, J.; Millera, A.; Bilbao, R.; Alzueta, M. U. *Combust. Flame* **2010**, *157* (2), 267−276.

(51) Chan, L. K.; Sarofim, A. F.; Beer, J. M. *Combust. Flame* **1983**, *52* (1), 37−45.

(52) Aarna, I.; Suuberg, E. M. *Energy Fuels* **1999**, *13* (6), 1145−1153.

(53) Tullin, C. J.; Sarofim, A. F.; Beer, J. M. *J. I. Energy* **1993**, *66* (469), 207−215.

(54) Wang, Z. H.; Zhou, J. H.; Wen, Z. C.; Liu, J. Z.; Cen, K. *Energy Fuels* **2007**, *21* (4), 2038−2043.

(55) Wu, S. L.; Iisa, K. *Energy Fuels* **1998**, *12* (3), 457−463.

(56) Zhao, Z. B.; Qiu, J. S.; Li, W.; Li, B. Q. *Fuel* **2003**, *82* (8), 949−957.

(57) Zhong, B. J.; Zhang, H. S.; Fu, W. B. *Combust. Flame* **2003**, *132* (3), 364−373.

(58) Zevenhoven, R.; Hupa, M. *Fuel* **1998**, *77* (11), 1169−1176.

(59) Zhong, B. J.; Tang, H. *Combust. Flame* **2007**, *149* (1−2), 234−243.

(60) Molina, A.; Eddings, E. G.; Pershing, D. W.; Sarofim, A. F. *Proc. Combust. Inst.* **2002**, *29*, 2275−2281.

(61) Basu, P. *Chem. Eng. Sci.* **1999**, *54* (22), 5547−5557.

(62) Gayan, P.; Adanez, J.; de Diego, L. F.; Garcia-Labiano, F.; Cabanillas, A.; Bahillo, A.; Aho, M.; Veijonen, K. *Fuel* **2004**, *83* (3), 277−286.